



CHORUS

This is the accepted manuscript made available via CHORUS. The article has been published as:

Density Functional Resonance Theory of Unbound Electronic Systems

Daniel L. Whitenack and Adam Wasserman

Phys. Rev. Lett. **107**, 163002 — Published 14 October 2011

DOI: [10.1103/PhysRevLett.107.163002](https://doi.org/10.1103/PhysRevLett.107.163002)

Density Functional Resonance Theory of Unbound Electronic Systems

Daniel L. Whitenack*

Department of Physics, Purdue University, 525 Northwestern Avenue, West Lafayette, IN 47907, USA

Adam Wasserman†

*Department of Chemistry, Purdue University, 560 Oval Drive, West Lafayette, IN 47907, USA and
Department of Physics, Purdue University, 525 Northwestern Avenue, West Lafayette, IN 47907, USA*

Density Functional Resonance Theory (DFRT) is a complex-scaled version of ground-state Density Functional Theory (DFT) that allows one to calculate the in-principle exact resonance energies and lifetimes of metastable anions. In this formalism, the energy and lifetime of the lowest-energy resonance of unbound systems is encoded into a complex “density” that can be obtained via complex-coordinate scaling. This complex density is used as the primary variable in a DFRT calculation just as the ground-state density would be used as the primary variable in DFT. As in DFT, there exists a mapping of the N -electron interacting system to a Kohn-Sham system of N non-interacting particles. This mapping facilitates self consistent calculations with an initial guess for the complex density, as illustrated with an exactly-solvable model system.

Density Functional Theory (DFT) [1–3] provides one of the most accurate and reliable methods to calculate the ground-state electronic properties of molecules, clusters, and materials from first principles. It is one of the workhorses of computational quantum chemistry [4]. In addition, DFT’s time-dependent extension (TDDFT) [5] can now be applied to a wealth of excited-state and time-dependent properties in both linear and non-linear regimes [6]. When the N -electron system of interest has no bound ground state, however, neither DFT nor TDDFT can be applied in a straightforward way to calculate properties of long lived metastable states such as resonance energies and lifetimes. A correct DFT calculation converges to the true ground state by ionizing the system, thus leaving no reliable starting point for a subsequent TDDFT calculation on the N -electron system. In practice, a finite simulation box or basis set can make the system artificially bound [7, 8], but information about the relevant lifetimes is lost in the process.

We address here this fundamental limitation of ground-state DFT, and propose a solution.

Consider a system of N interacting electrons in an external potential $\tilde{v}(\mathbf{r})$, with a ground-state electron density $\tilde{n}(\mathbf{r}) = \langle \tilde{\Psi}^0 | \hat{n}(\mathbf{r}) | \tilde{\Psi}^0 \rangle$ where $|\tilde{\Psi}^0\rangle$ is the many-body ground state wavefunction and $\hat{n}(\mathbf{r}) = \sum_{i=1}^N \delta(\mathbf{r} - \hat{\mathbf{r}}_i)$ is the density operator. The potential, $\tilde{v}(\mathbf{r})$, is set to be everywhere positive and go to a positive constant C as $|\mathbf{r}| \rightarrow \infty$ such that $\tilde{v}(\mathbf{r})$ can support a bound ground state with energy $\tilde{E} > 0$. Next we ask how the ground-state electron density changes when a smooth step is added to $\tilde{v}(\mathbf{r})$ at a radius $|\mathbf{R}|$ that is larger than the range of $\tilde{v}(\mathbf{r})$. The step is such that the new potential $v(\mathbf{r})$ coincides with $\tilde{v}(\mathbf{r})$ for $|\mathbf{r}| < |\mathbf{R}|$ but goes to zero at infinity instead of going to a positive constant. Since $v(\mathbf{r})$ is everywhere positive and goes to zero at infinity, all N electrons tunnel out of the steps and $v(\mathbf{r})$ supports no bound states. The correct ground state energy $E \rightarrow 0^+$ as all electrons leave the system with zero kinetic energy, and the new density,

$n(\mathbf{r})$, is delocalized through all space. In practical calculations, however, $v(\mathbf{r})$ and $\tilde{v}(\mathbf{r})$ cannot be distinguished if $|\mathbf{R}|$ is beyond the size of the simulation box. The result provided by ground-state DFT with such a simulation box and using the *exact* exchange-correlation functional (which should give the in-principle exact ground-state energy) is not E , but $\tilde{E} > 0$, and the density obtained is $\tilde{n}(\mathbf{r})$ as if the system were bound. Even when the simulation box is large enough to include the steps, use of a finite basis-set of localized functions will artificially bind all electrons. Clearly, such calculations do not provide approximations to the true ground-state energy and density of $v(\mathbf{r})$, but to those of its lowest-energy resonance (LER).

The purpose of this letter is to establish an analog of KS-DFT that provides the in-principle exact LER-density along with its energy and lifetime for any finite $|\mathbf{R}|$. This analog is motivated by the one-to-one mapping between *complex-scaled* external potentials and the associated *complex* LER density functions [9]. As $|\mathbf{R}| \rightarrow \infty$, the results coincide with those of standard KS-DFT. For higher-energy resonances, TDDFT is needed as a matter of principle [10, 11].

First, we note that as $|\mathbf{R}| \rightarrow \infty$, the complex density $n_\theta(\mathbf{r})$ associated with the LER of

$$\hat{H}_v = \hat{T} + \hat{V}_{ee} + \int d\mathbf{r} \hat{n}(\mathbf{r}) v(\mathbf{r}) \quad , \quad (1)$$

becomes equal to the complex density $\tilde{n}_\theta(\mathbf{r})$ associated to $\tilde{v}(\mathbf{r}e^{i\theta})$. In Eq. 1, $\hat{T} = -\frac{1}{2} \sum_{i=1}^N \nabla_i^2$ is the kinetic energy operator and $\hat{V}_{ee} = \sum_{i,j \neq i}^N |\mathbf{r}_i - \mathbf{r}_j|^{-1}$ is the electron-electron interaction (atomic units are used throughout). To find $n_\theta(\mathbf{r})$, we complex-scale \hat{H}_v by multiplying all electron coordinates by the phase factor $e^{i\theta}$, diagonalize the resulting non-hermitian operator \hat{H}_v^θ , and calculate the bi-expectation value of $\hat{n}(\mathbf{r})$ as:

$$n_\theta(\mathbf{r}) = \langle \Psi_\theta^L | \hat{n}(\mathbf{r}) | \Psi_\theta^R \rangle \quad , \quad (2)$$

where $|\Psi_\theta^R\rangle$ and $\langle\Psi_\theta^L|$ are the right and left eigenstates corresponding to the complex eigenvalue of \hat{H}_v^θ that has the smallest positive real part among all eigenvalues in the non-rotating spectrum of \hat{H}_v^θ . For a detailed review of this technique and related methods in non-hermitian Quantum Mechanics, see ref. [12, 13]. The computational cost of this prescription scales exponentially with the number of particles. Since $n_\theta(\mathbf{r}) \rightarrow \tilde{n}_\theta(\mathbf{r})$ as $|\mathbf{R}| \rightarrow \infty$, and since there is a one-to-one correspondence between $n_\theta(\mathbf{r})$ and $v(\mathbf{r}e^{i\theta})$ [9, 14], the complex energy of the LER is a functional of n_θ , $E_\theta[n_\theta]$, and goes to \tilde{E} (not E), as $|\mathbf{R}| \rightarrow \infty$. Its lifetime \mathcal{L} is given by $(-2\text{Im}(E_\theta))^{-1}$, and for any finite $|\mathbf{R}|$,

$$E_\theta[n_\theta] = \mathcal{E}[n_\theta] - \frac{i}{2}\mathcal{L}^{-1}[n_\theta] \quad , \quad (3)$$

where the resonance energy \mathcal{E} tends to \tilde{E} as $|\mathbf{R}| \rightarrow \infty$. According to the complex variational principle of Ref. [9], the one-to-one mapping between $n_\theta(\mathbf{r})$ and $v(\mathbf{r}e^{i\theta})$ applies to complex densities that can be obtained via Eq. 2 from an antisymmetric N -electron wavefunction (i.e. they are N -representable complex densities).

To build a complex analog of Kohn-Sham DFT using $n_\theta(\mathbf{r})$ as the basic variable, we first map the system of interacting electrons (whose LER density is $n_\theta(\mathbf{r})$) to one of N particles moving independently in a complex ‘‘Kohn-Sham’’ potential, $v_s^\theta(\mathbf{r})$, defined such that its N occupied complex orbitals $\{\phi_i^\theta(\mathbf{r})\}$ yield the interacting LER-density via $n_\theta(\mathbf{r}) = \sum_{i=1}^N \langle \phi_i^{\theta,L} | \hat{n}(\mathbf{r}) | \phi_i^{\theta,R} \rangle$. In Moiseyev’s Hermitian representation of complex-scaling [15], the complex Kohn-Sham equations are:

$$\begin{pmatrix} \hat{h}_1 - \varepsilon_i & -\hat{h}_2 - 2\tau_i^{-1} \\ \hat{h}_2 + 2\tau_i^{-1} & \hat{h}_1 - \varepsilon_i \end{pmatrix} \begin{pmatrix} \text{Re}(\phi_i^\theta) \\ \text{Im}(\phi_i^\theta) \end{pmatrix} = 0 \quad , \quad (4)$$

where $\hat{h}_1 = -\frac{1}{2}\cos(2\theta)\nabla^2 + \text{Re}(v_s^\theta(\mathbf{r}))$, and $\hat{h}_2 = \frac{1}{2}\sin(2\theta)\nabla^2 + \text{Im}(v_s^\theta(\mathbf{r}))$. The set of $\{\varepsilon_i\}$ and $\{\tau_i\}$ provide the orbital resonance energies and lifetimes of the Kohn-Sham particles.

Second, we write $E_\theta[n_\theta]$ as:

$$E_\theta[n_\theta] = T_s^\theta[n_\theta] + \int d\mathbf{r} n_\theta(\mathbf{r})v(\mathbf{r}e^{i\theta}) + E_H^\theta[n_\theta] + E_{\text{xc}}^\theta[n_\theta] \quad (5)$$

in analogy to standard KS-DFT, and require: $T_s^\theta[n_\theta] = e^{-2i\theta}T_s[n_\theta]$ and $E_H^\theta[n_\theta] = e^{-i\theta}E_H[n_\theta]$, where $T_s[n_\theta]$ and $E_H[n_\theta]$ are the standard non-interacting kinetic and Hartree functionals evaluated at the complex densities. Without an explicit expression for $E_{\text{xc}}^\theta[n_\theta]$, however, the total energy cannot be calculated via Eq. 5. Related work by Ernzerhof [14] and physical intuition suggest that bound ground-state functionals are applicable here. They are, in any case, the most natural candidates. Eq. 5 then defines $E_{\text{xc}}^\theta[n_\theta]$. The complex variational principle [13] along with the assumption that the orbitals used to

construct the density can be expanded in an orthonormal basis leads to the Euler-Lagrange equation:

$$\frac{\delta E_\theta[n_\theta]}{\delta n_\theta} - \mu \int d\mathbf{r} n_\theta(\mathbf{r}) = 0 \quad . \quad (6)$$

Performing the variation in Eq. 5 and comparing with Eq. 4 leads to an expression for the Kohn-Sham potential that is again analogous to that of standard KS-DFT:

$$v_s^\theta(\mathbf{r}) = v(\mathbf{r}e^{i\theta}) + e^{-i\theta}v_H[n_\theta](\mathbf{r}) + v_{\text{xc}}^\theta[n_\theta](\mathbf{r}) \quad , \quad (7)$$

where $v_{\text{xc}}^\theta[n_\theta](\mathbf{r}) = \delta E_{\text{xc}}^\theta[n_\theta]/\delta n_\theta(\mathbf{r})|_{\text{LER}}$.

The simplest case where all essential aspects of this formalism can be illustrated is a system of two interacting electrons moving in a one-dimensional potential that supports only metastable states. We study a Hamiltonian where the electrons interact via a soft-Coulomb potential of strength λ :

$$\hat{H} = \sum_{i=1}^2 \left[-\frac{1}{2} \frac{d^2}{dx_i^2} + v(x_i) \right] + \frac{\lambda}{\sqrt{1 + (x_1 - x_2)^2}} \quad , \quad (8)$$

using $v(x) = a \left[\sum_{j=1}^2 \left(1 + e^{-2c(x+(-1)^j d)} \right)^{-1} - e^{-\frac{x^2}{b}} \right]$. Its

parent potential $\tilde{v}(x) = a(1 - e^{-x^2/b})$ goes to a as $x \rightarrow \pm\infty$, but $v(x)$ goes down to zero at $x \sim \pm d$.

Exact solution via the 2-electron wavefunction: The complex-scaled Hamiltonian $\hat{H}_\theta = \hat{H}(\{x_i\} \rightarrow \{x_i e^{i\theta}\})$ was diagonalized with the Fourier Grid Hamiltonian (FGH) [16] and Finite Difference Methods. The numerically exact $n_\theta(x)$ was calculated via Eq. 2. The complex density $n_\theta(x)$ depends on the value of θ (see Fig. 1), but for a large enough number of grid points the energy does not. In the complex-scaling method the resonance energies are precisely those that remain stationary as θ changes [13]. Fig. 2 shows the energy for $0 < \lambda < 1$.

Exact KS solution: Two non-interacting electrons in the potential indicated by solid lines in Fig.3 have the same $n_\theta(x)$ as calculated above to one part in 10^6 (in the sense that the space integral of the square of the difference between their real or imaginary parts is less than 10^6). When $n_\theta(x)$ is set to integrate to the number of electrons (2, here), we verify this potential is given by:

$$v_s^\theta(x) = e^{-2i\theta} \frac{\nabla^2 \sqrt{n_\theta(x)}}{2\sqrt{n_\theta(x)}} - \varepsilon_H + 2i\tau_H^{-1} \quad , \quad (9)$$

where $\varepsilon_H - 2i\tau_H^{-1}$ is the highest occupied complex orbital energy (in this case the only one). This is in exact analogy to real KS-potentials for bound 2-electron systems where Eq. 9 follows from taking the first functional derivative of the Von-Weizsacker functional [17].

Exchange: For 2-electron systems, the exchange functional is known in terms of the classical Hartree functional, and Eqs. 4 and 7 were solved employing $E_{\text{x}}^\theta[n_\theta] =$

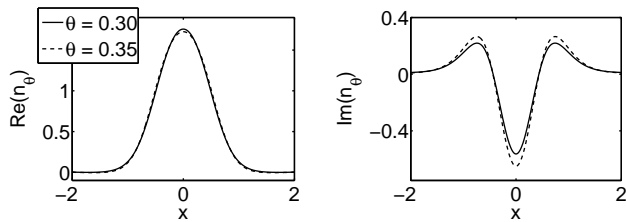


FIG. 1. Exact 2-electron complex densities associated with the LER of $v(x)$ when using different scaling angles ($a = 4$, $b = 0.5$, $c = 4$, $d = 2$, and $\lambda = 1$).

$-\frac{1}{2}E_{\text{H}}^{\theta}[n_{\theta}] = -\frac{1}{2}e^{-i\theta}E_{\text{H}}[n_{\theta}]$. The complex KS equations can be solved self-consistently with an initial guess for n_{θ} . Starting with the non-interacting complex density, the SCF calculations converged in 4-5 iterations. The resulting complex energies are plotted in Fig. 2 along with the exact results. For comparison we also plot the results from calculating the first order perturbation theory correction to the exact solution of the complex-scaled 2-electron problem. The latter two yield identical answers for the resonance energies, and extremely close answers for the lifetimes for all λ in the range $0 < \lambda < 1$. Thus, neglecting correlation, we find the average error is $\sim 14\%$ for the real part and $\sim 35\%$ for the imaginary part of the total energy. We also compare with standard scattering calculations using the close-coupling equations under the bound state approximation [18, 19]. The resonance energy is predicted by this method with an error of 22%, comparable to our DFRT exchange-only results.

As in standard KS-DFT, total energies are given by:

$$E_{\theta}[n_{\theta}] = \sum_{i=1}^N (\varepsilon_i - 2i\tau_i^{-1}) + E_{\text{HX}}^{\theta}[n_{\theta}] - \int d\mathbf{r} v_{\text{HX}}^{\theta} n_{\theta}(\mathbf{r}) \quad (10)$$

We point out that the θ -independence of the energy is preserved by the SCF procedure (see Table I). As the grid-size increases the dependence on θ becomes negligible. This is important, because within a SCF DFRT calculation one is always solving the 1-body complex KS equations. For these equations, one should be able to efficiently use a large enough basis set or a fine enough grid to extinguish most of the numerical θ dependence. Thus, this well-known drawback of the complex-scaling technique [20–22] is outdone by the benefit of never having to deal with N -particle wavefunctions, but just 1-body (complex) densities.

Correlation: It is of interest to calculate the exact correlation potential, which we do by subtracting the hartree-exchange contribution from the exact KS potential. The individual Hartree-exchange and correlation potentials are shown in Fig. 4. To interpret the features in these complex potentials it is useful to distinguish between two regions. As the interaction between

Grid	θ	Re(E)	Im(E)
(N = 299)	0.27	4.99895	-0.0149586
	0.35	4.99933	-0.0144161
	0.43	4.99962	-0.0139792
(N = 1299)	0.27	5.00182	-0.0161045
	0.35	5.00198	-0.0159848
	0.43	5.00200	-0.0159513

TABLE I. Two-electron resonance energy values in the model Hamiltonian of Eq. 8 calculated via exchange-only DFRT. As the grid spacing decreases numerical dependence on θ practically disappears. ($a = 4$, $b = 0.5$, $c = 4$, $d = 2$ and $\lambda = 1$)

electrons is turned on and λ increases from 0 to 1, the region around the central well is shifted up in the real part of the Kohn-Sham potential. This behavior is also seen in standard KS-DFT, and serves to shift up the position of the non-interacting orbital energies (in that case their real part). However, both the real and imaginary part of the complex Kohn-Sham potential have a second region outside the central well that shows a dramatic oscillatory structure arising purely from the fact that the state is unbound. It is already known that the decaying oscillations in the tails of the complex LER wavefunction are governed by the lifetime of the resonance [23]. These oscillations serve to produce the correct asymptotic behavior in the interacting complex density.

Orbital Energies: Although the ionization energy of our 2-electron system is strictly zero, it is tempting to define $I_{\theta} \equiv E_{\theta}(N = 1) - E_{\theta}(N = 2)$ and check whether it equals minus the highest occupied KS orbital energy, as Koopmans' theorem for DFT would suggest. For the parameters used in Figs.1-4, $E_{\theta}(N = 1) = 1.629 - 0.003i$, $E_{\theta}(N = 2) = 4.127 - 0.014i$, but the exact KS eigenvalue is $2.065 - 0.006i$. Therefore, in this case the HOMO energy of the KS system is not equal to $-I_{\theta}$. This occurs because there is more than one decay channel. When the decay is restricted to a single channel the HOMO energy can be related to the difference between the metastable complex LER energy and the threshold energy. For example, in a system like N_2^- that decays to N_2 , the HOMO energy of DFRT equals $(-A - (\Gamma/2)i)$ where A is the negative electron affinity of N_2 (or the ionization potential of N_2^-) and Γ is the width of the N_2^- resonance. Note that for purely bound ground states $\Gamma = 0$ and one recovers Koopmans' theorem for DFT.

We are working on the implementation of DFRT to calculate the lifetime of molecular metastable anions. The method is also applicable to molecules connected to metallic leads, as in molecular electronics. Ernzerhof and co-workers have developed an approach for that purpose where complex absorbing potentials are added within a complex-DFT framework [14, 24]. However, we emphasize that the complex potentials in DFRT are the result of a variational calculation, and they are obtained

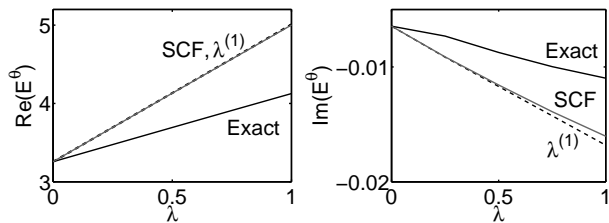


FIG. 2. The real and imaginary parts of E_θ in the model Hamiltonian of Eq. 8 calculated exactly with complex scaling, a first order correction to the non-interacting energy, and our DFRT exchange-only self-consistent method. ($a = 4$, $b = 0.5$, $c = 4$, $d = 2$, and $\lambda = 1$)

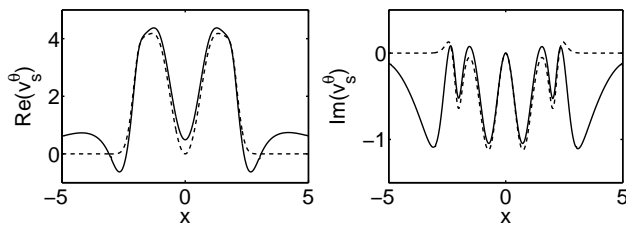


FIG. 3. The real and imaginary part of the complex KS potential for the LER of 2 soft-Coulomb interacting electrons in the model potential, Eq.8. The dashed lines are the real and imaginary part of the complex-scaled parent potential $\tilde{v}(x)$. ($\theta = 0.35$, $a = 4$, $b = 0.5$, $c = 4$, $d = 2$, and $\lambda = 1$).

self-consistently for the N -electron system treated as isolated, rather than added to the Hamiltonian from the start to model an open system.

DFRT should also be applicable to study shape and Feshbach resonances in low-energy electron scattering processes [25–27] of growing interest in biological systems [28–30], atmospheric sciences, lasers, and astrophysics [31–34].

In summary, DFRT provides an unambiguous prescription for calculating negative electron affinities based on a complex-scaled version of standard ground state DFT. This complex-scaled version has been cast in a way that is analogous in practice to KS-DFT. Results on a model system suggest that the same machinery that has been developed for KS-DFT yields accurate resonance energies and lifetimes in DFRT. It remains to be seen if common approximations to $E_{xc}[n]$ are able to capture the important effects that determine properties of real transient anions. A more detailed study of the complex density function and various DFRT identities is forthcoming.

In addition to the varied practical applications of the formalism, DFRT provides a more general theoretical framework than DFT itself. DFRT allows one to calculate both bound and unbound properties, but it reduces to standard DFT when the complex transformation is removed. Due to this link, DFRT can be used as a tool to shed light on DFT and TDDFT. For example, one

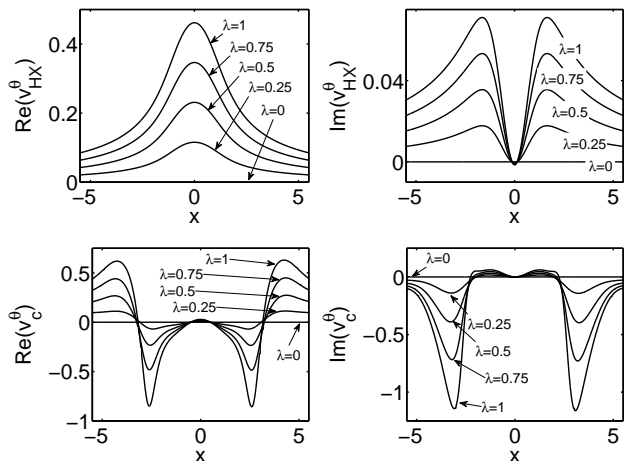


FIG. 4. The individual contributions to the Kohn-Sham potential from Hartree-exchange and correlation. ($\theta = 0.35$, $a = 4$, $b = 0.5$, $c = 4$, $d = 2$, and $\lambda = 1$)

can explore exact properties of functionals, such as integer discontinuities, across a wide range of both bound and unbound systems; the response of the complex density could reveal metastable excitations previously hidden in standard linear response TDDFT; derivatives of the complex density function could extend chemical reactivity theory to metastable systems. Therefore, DFRT promises new perspective on many active research areas in the quantum theory of many-body systems.

Acknowledgment is made to the Donors of the American Chemical Society Petroleum Research Fund for support of this research under grant No.PRF# 49599-DNI6.

* dwhitena@purdue.edu; <http://www.purdue.edu/dft>

† awasser@purdue.edu

- [1] P. Hohenberg and W. Kohn, Phys. Rev. **136**, B864 (1964).
- [2] W. Kohn and L. J. Sham, Phys. Rev. **140**, A1133 (1965).
- [3] R. G. Parr and W. Yang, *Density-Functional Theory of Atoms and Molecules* (Oxford University Press, Oxford, 1994).
- [4] R. M. Martin, *Electronic Structure: Basic Theory and Practical Methods* (Cambridge University Press, London, 2004).
- [5] E. Runge and E. K. U. Gross, Phys. Rev. Lett. **52**, 997 (1984).
- [6] M. A. L. Marques, C. A. Ullrich, F. Nogueira, A. Rubio, K. Burke, and E. K. U. Gross, *Time-Dependent Density Functional Theory* (Springer, Verlag Berlin Heidelberg, 2006).
- [7] D. Lee, F. Furche, and K. Burke, J. Phys. Chem. Lett. **1**, 2124 (2010).
- [8] M. Kim, E. Sim, and K. Burke, J. Chem. Phys. **134**, 171103 (2011).
- [9] A. Wasserman and N. Moiseyev, Phys. Rev. Lett. **98**,

- 093003 (2007).
- [10] A. J. Krueger and N. T. Maitra, *Phys. Chem. Chem. Phys.* **11**, 4655 (2009).
- [11] M. van Faassen and K. Burke, *J. Chem. Phys.* **124**, 094102 (2006); *Chem. Phys. Lett.* **431**, 410 (2006); *Phys. Chem. Chem. Phys.* **11**, 4437 (2009).
- [12] D. L. Whitenack and A. Wasserman, *J. Phys. Chem. Lett.* **1**, 407 (2010).
- [13] N. Moiseyev, *Non-Hermitian Quantum Mechanics* (Cambridge University Press, London, 2011).
- [14] M. Ernzerhof, *J. Chem. Phys.* **125**, 124104 (2006).
- [15] N. Moiseyev, *Phys. Chem. Lett.* **99**, 364 (1983).
- [16] S. Chu, *Chem. Phys. Lett.* **167**, 155 (1990).
- [17] C. F. von Weizsacker, *Z. Phys.* **96**, 431 (1935).
- [18] S. K. Adhikari, *Variational Principles and the Numerical Solution of Scattering Problems* (John Wiley and Sons, Inc., New Jersey, 1998).
- [19] J. R. Taylor, *Scattering Theory* (Dover Publications, Inc., New York, 1972).
- [20] N. Moiseyev, P. R. Certain, and F. Weinhold, *Mol. Phys.* **36**, 1613 (1978).
- [21] W. P. Reinhardt, *Ann. Rev. Phys. Chem.* **33**, 223 (1982).
- [22] B. Simon, *Ann. Math.* **97**, 247 (1973).
- [23] U. Peskin, N. Moiseyev, and R. Lefebvre, *J. Chem. Phys.* **92**, 2902 (1990).
- [24] F. Goyer, M. Ernzerhof, and M. Zhuang, *J. Chem. Phys.* **126**, 144104 (2007).
- [25] R. E. Palmer and P. J. Rous, *Rev. Mod. Phys.* **64**, 383 (1992).
- [26] J. Simons, *J. Phys. Chem. A* **112**, 6401 (2008); *Annu. Rev. Phys. Chem.* **67**, 107 (2011).
- [27] T. A. Field, K. Graupner, A. Mauracher, P. Scheier, A. Bacher, S. Denifl, F. Zappa, and T. D. Mark, *J. Phys.: Conf. Ser.* **88**, 012029 (2007).
- [28] X. Pan, P. Cloutier, D. Hunting, and L. Sanche, *Phys. Rev. Lett.* **90**, 208102 (2003).
- [29] X. Pan and L. Sanche, *Phys. Rev. Lett.* **94**, 198104 (2005).
- [30] M. Mucke, M. Braune, S. Barth, M. Frstel, T. Lischke, V. Ulrich, T. Arion, U. Becker, A. Bradshaw, and U. Hergenbahn, *Nature Physics* **6**, 143 (2010).
- [31] H. S. W. Massey, *Negative Ions* (Cambridge University Press, London, 1950).
- [32] W. Liang¹, M. P. Shores, M. Bockrath, J. R. Long, and H. Park, *Nature* **417**, 725 (2002).
- [33] V. Strelkov, *Phys. Rev. Lett.* **104**, 123901 (2010).
- [34] R. Olivares-Amaya, M. Stopa, X. Andrade, M. A. Watson, and A. Aspuru-Guzik, *J. Phys. Chem. Lett.* **2**, 682 (2011).